Elastic anomalies in $(V_{1-x}Cr_x)_2O_3$: Electron-transfer effects

H. Yang and R. J. Sladek
Department of Physics, Purdue University, West Lafayette, Indiana 47907
(Received 17 March 1986)

Transit times of 30-MHz ultrasonic waves in $(V_{1-x}Cr_x)_2O_3$ single crystals with nominal x values of 0.015 and 0.03 were measured as a function of temperature between 300 and 650 K. The results were used to determine the temperature dependence of the elastic constants. C_{11} and C_{12} each go through a broad minimum centered at about 560 K while C_{13} exhibits a similar but much shallower minimum. On the other hand, C_{33} decreases nonlinearly with increasing temperature but has a change in slope where C_{11}, C_{12}, and C_{13} go through their lowest values. It is found that the anomalous components of these $C_{\mu\nu}$'s can be attributed to the electronic contributions involving the ultrasonic-strain-induced transfer of $3d$ electrons between $e_g(\pi)$ subbands which are separated by a temperature-dependent energy gap. It is also found that this electron-transfer mechanism can account for some of the anomalous pressure dependences of the elastic constants reported earlier.

I. INTRODUCTION

$(V_{1-x}Cr_x)_2O_3$ is a system of compounds which exhibit structural, magnetic, and/or electric transitions accompanying changes in temperature, pressure, or composition.[1,2] The greatly different behavior of the electrical resistivity and the lattice parameters of V_2O_3 containing a small amount of Cr_2O_3 from that of pure V_2O_3 has been the subject of experimental and theoretical investigations, especially in regard to the broad, electrical transition which occurs between about 350 and 700 K without any change in crystal symmetry.[3-5] The origin of this high-temperature transition in pure and Cr-doped V_2O_3 has been discussed in terms of changes in the electronic energy bands[3,6] arising mainly from the $3d$ levels of the metal ions. Zeiger[6] developed a a_{1g}-e_g band-edge crossing model to interpret the high-temperature electrical transition in $(V_{1-x}Cr_x)_2O_3$ while Kuwamoto *et al.*[3] suggested the presence of a temperature-dependent energy gap in the semiconducting phase of $(V_{1-x}Cr_x)_2O_3$ with $0.006<x<0.03$. More recent band-structure calculations[7,8] suggest that in V_2O_3 the Fermi energy (E_F) is located within the one-quarter-filled e_g band while the full, lower-lying a_{1g} band makes a negligible contribution to the total density of states at E_F.

Nichols *et al.*[9] have measured the elastic constants, $C_{\mu\nu}$, of V_2O_3 and found that striking anomalies accompany the high-temperature electrical transition. An attempt to attribute these elastic anomalies to electronic effects was unsuccessful partly because of the difficulty in separating out the lattice contributions to the $C_{\mu\nu}$'s due to unusual changes in the lattice parameters.[2,4,5] In this work we have extended the $C_{\mu\nu}$ versus T measurements to semiconducting $(V_{1-x}Cr_x)_2O_3$ crystals with $x=0.015$ and/or 0.03 which do not suffer from thermal expansion anomalies[5,10] with the hope of gaining insight into the electronic contributions to the elastic properties at high temperatures.

II. EXPERIMENTAL PROCEDURE

We used the same samples as in our previous investigations.[11,12] They were obtained from single-crystal boules of $(V_{1-x}Cr_x)_2O_3$ with $x=0.015$ and 0.03. The boules were grown in the Central Materials Preparation Facility of the Purdue University Materials Research Laboratory utilizing the skull-melting technique.[13] The actual Cr fractions were determined by a commercial atomic absorption analysis[14] to be 0.013 and 0.027, respectively, for the samples with nominal compositions of 0.015 and 0.03.

Transit times τ_i of various 30-MHz ultrasonic waves were measured every few degrees in the temperature range from 300 K up to 650 K by means of the pulse-echo-overlap technique.[15] Dow Corning 805 resin, dissolved in xylene and mixed with Permatex gasket shellac compound, was used in bonding X-cut and AC-cut quartz transducers to the sample. Temperatures were achieved by means of a furnace surrounding the quartz tube encasing the sample holder and were determined by a Chromel-Alumel thermocouple. In order to prevent oxidation of our samples the measurements were performed under gettered argon.

The six independent elastic constants were determined from seven elastic stiffness moduli, ρv_i^2 ($v_i=2L/\tau_i$) where ρ is the density and L the sample length, by least-squares fits to equations[9] relating the $C_{\mu\nu}$'s to the ρv_i^2's. Corrections to the elastic moduli due to changes in sample length and density with temperature were neglected since they were less than 0.5% even at 650 K.

III. RESULTS

Although we determined all six independent $C_{\mu\nu}$'s for our $(V_{0.985}Cr_{0.015})_2O_3$ sample between 300 and 650 K, only the elastic constants C_{11}, C_{33}, C_{12}, and C_{13} are plotted as a function of temperature in Fig. 1 because the remaining elastic constants, C_{44} and C_{14}, do not have any pronounced temperature dependence associated with the

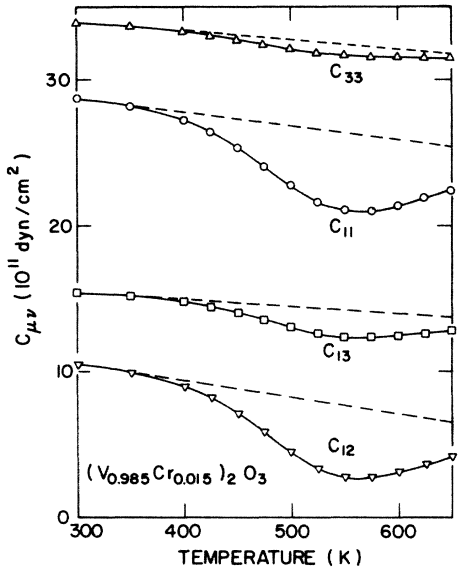

FIG. 1. Experimental elastic constants C_{11}, C_{12}, C_{13}, and C_{33} between 300 and 650 K for $(V_{0.985}Cr_{0.015})_2O_3$. The dashed curves represent the "background" elastic constants, $C^B_{\mu\nu}$, obtained as described in the text.

high-temperature electrical transition. It should be mentioned, however, that we have already reported[11,16] on the anomalies softening of C_{44} and C_{14} in samples with $x=0.015$ and/or 0.03 as the low-temperature structural transition is approached from above. As can be seen in Fig. 1, C_{11} and C_{12} each goes through a broad minimum centered at about 560 K while C_{13} exhibits a similar but much shallower minimum. On the other hand, C_{33} decreases nonlinearly with increasing temperature but has a change in slope at about the same temperature where C_{11}, C_{12}, and C_{13} to through their lowest values. These temperature dependences are similar to, but substantially smaller than, those in pure V_2O_3 for which the minima occur at somewhat higher temperatures.[9]

In order to obtain a more quantitative description of the anomalous component of each elastic constant we used an expression [Eq. (1) below] based on an anharmonic-oscillator model[17] to deduce the ordinary of "background" elastic constant behavior expected in the absence of any phase transitions. Equation (1) should be suitable for this purpose since, unlike pure V_2O_3, $(V_{1-x}Cr_x)_2O_3$ crystals in the semiconducting phase do not exhibit any thermal expansion anomalies as was mentioned in the Introduction. The expression for the elastic constant, developed by Lakkad,[17] is given by

TABLE I. The values of the parameters $C^0_{\mu\nu}$ and $K_{\mu\nu}$ obtained by fitting Eq. (1) to the experimental elastic constants between 300 and 310 K and used to produce the dashed curves in Fig. 1 for $(V_{0.985}Cr_{0.015})_2O_3$.

$\mu\nu$	$C^0_{\mu\nu}$(10^{11} dyn/cm^2)	$K_{\mu\nu}$
11	30.1	0.19
33	34.8	0.11
12	12.2	0.59
13	16.1	0.19

$$C^{\text{anh}}_{\mu\nu}(T)=C^0_{\mu\nu}[1-K_{\mu\nu}F(T/\Theta_D)]\ , \tag{1}$$

where

$$F(T/\Theta_D)=3(T/\Theta_D)^4\int_0^{\Theta_D/T}x^3(e^x-1)^{-1}dx\ . \tag{2}$$

Here, $C^0_{\mu\nu}$ and $K_{\mu\nu}$ are constants developed on crystallographic orientation and Θ_D is the Debye temperature. By fitting these expressions with $\Theta_D=580$ K (Ref. 18) to the experimental data points in the temperature range $300<T<310$ K, where the effect of the transition seems to be extremely small, we have estimated the values of "background" elastic constant, $C^B_{\mu\nu}$, at higher temperatures. These $C^B_{\mu\nu}$'s are given by the dashed curves in Fig. 1. The values of $C^0_{\mu\nu}$ and $K_{\mu\nu}$ deduced from the least-squares fits are tabulated in Table I. The anomalous component of each elastic constant, $\Delta C_{\mu\nu}(T)$, is estimated by subtracting $C^B_{\mu\nu}(T)$ from the experimental $C_{\mu\nu}(T)$.

It can be seen that all the $\Delta C_{\mu\nu}$'s in Fig. 2 have generally similar temperature dependences with

$$\Delta C_{11}\simeq\Delta C_{12} \tag{3a}$$

and

$$\Delta C^*_{13}\equiv-\left[\left[\frac{\Delta C_{11}+\Delta C_{12}}{2}\right]\Delta C_{33}\right]^{1/2}\simeq\Delta C_{13}\ . \tag{3b}$$

The significance of these relations will be discussed in the next section.

IV. DISCUSSION

We propose that the anomalous temperature dependence of the $C_{\mu\nu}$'s in $(V_{0.985}Cr_{0.015})_2O_3$ are due to an electronic effect[19,20] involving ultrasonic-strain-induced transfer of electrons between $3d$ subbands. Before discussing this mechanism in detail, we note that the internal-strain contribution[21–23] can not be responsible for the elastic anomalies in $(V_{0.985}Cr_{0.015})_2O_3$ since it has the form $-g^2/\omega_R^2$ and neither g, the coupling constant between the optical and acoustic displacements, nor ω_R, the Raman-mode frequency, is expected to have an appropriate temperature dependence in the temperature range of our interest. This is known to be true for ω_R from recent

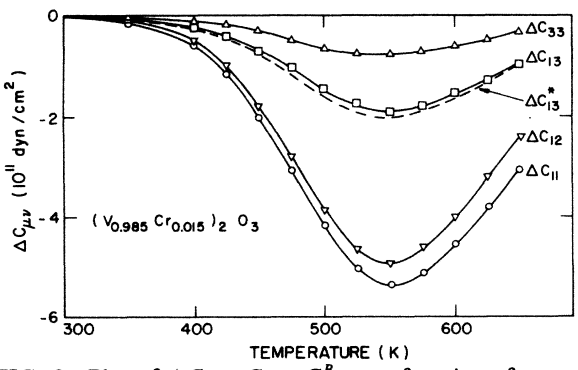

FIG. 2. Plot of $\Delta C_{\mu\nu}=C_{\mu\nu}-C^B_{\mu\nu}$ as a function of temperature between 300 and 650 K for $(V_{0.985}Cr_{0.015})_2O_3$. $-\Delta C^*_{13}$ is the geometrical average of $(\Delta C_{11}+\Delta C_{12})/2$ and ΔC_{33} as defined in Eq. (3b).

Raman-spectra measurements above room temperature[24] and may also be true for g because of the absence of any anomalies in the thermal expansion. On the other hand, it is interesting to note that there is a softening with subsequent partial recovery in the frequency of each A_{1g} Raman mode in pure V_2O_3.[24] This together with the unusual temperature dependences in the lattice parameters and atomic separations[4,5] suggest that the internal-strain mechanism might be responsible for at least part of the $C_{\mu\nu}$ versus T anomalies observed in V_2O_3 (Ref. 9).

We are now in a position to discuss if and how the electrical properties of $(V_{1-x}Cr_x)_2O_3$ crystals in the semiconducting phase can be used to interpret our elastic data. Honig and co-workers,[3] from their extensive measurements of electrical resistivity and Seebeck coefficient of $(V_{1-x}Cr_x)_2O_3$ crystals, deduced the energy gap as a function of temperature from 300 K up to 500 K using a simple two-band semiconductor model. Quite interestingly, the energy gap curves were found to be almost identical for samples with x between 0.006 and 0.03. This is shown by the solid curve in Fig. 3. Furthermore, they proposed a phenomenological picture for the density of states to interpret qualitatively the transition from metallic to semiconducting behavior which occurs in V_2O_3 as a result of doping with Cr_2O_3. More recent calculations[7,8] of the $3d$-band density of states of V_2O_3 also reveals a deep minimum between two $e_g(\pi)$ subbands where the Fermi level is located.

In view of the above-mentioned considerations we assume that in $(V_{0.985}Cr_{0.015})_2O_3$ two narrow subbands, $e_g^1(\pi)$ and $e_g^2(\pi)$, are separated by an energy gap of 0.31 eV (Ref. 3) at room temperature with the Fermi level lying half way in between. As the temperature increases, the peak-to-peak distance of 0.4 eV (Ref. 8) will be maintained while each subband broadens in a manner so as to result in the energy gap shown in Fig. 3. This will eventually lead to an overlap between the two subbands above 500 K. However, since the extent to overlap cannot be estimated, we have chosen the energy gap above 500 K in such a way as to optimize the agreement between computed and experimental $\Delta C_{\mu\nu}$'s. This yielded a different value of energy gap for each of our samples at a given temperature above 500 K (dashed curves in Fig. 3). It is noted that the above procedure for choosing the energy gap for $T > 500$ K seems to require an unreasonably large broadening of each subband. To avoid this situation one could assume that the change in the electronic band structure with temperature is due to a combination of broadening and rigid shifting of the bands toward each other rather than band broadening alone. However, this is not expected to be important for estimating the electronic contributions to the elastic constants. In calculating the electron-transfer contribution to the $C_{\mu\nu}$'s as a function of temperature we used a deformation-potential approximation[19] in which the shift of the $e_g^1(\pi)$ subband relative to the $e_g^2(\pi)$ subband due to ultrasonic strain is given by

$$\delta E = \sum_{\mu} A_\mu \epsilon_\mu \ , \tag{4}$$

where A_μ and ϵ_μ are the μth component ($\mu = 1$ to 6 in Voigt's notation) of the deformation potential and strain, respectively. We assume for our corundum-structured crystals that only terms of Eq. (4) involving A_1, A_2, and A_3 are nonzero and that $A_1 = A_2$ (Ref. 20). The electronic free-energy density of this two-band system (neglecting the contributions from the other bands relatively distant from the Fermi level) can be written as[19]

$$F_{\rm el} = \sum_{i=1}^{2} \int n^{(i)}(E) \left[E_F f(E,E_F) + \frac{1}{\beta} \ln[1 - f(E,E_F)] \right] dE \ , \tag{5}$$

where $\beta = 1/kT$, $f(E,E_F) = \{\exp[\beta(E - E_F)] + 1\}^{-1}$, and $n^{(i)}(E)$ is the density of states for the ith band. For simplicity, we assume that each band has a density of states given by

$$n(E) \propto W^{-3/2}(E - E^2/W)^{1/2} \ ,$$

where W is the bandwidth. It should be mentioned that a preliminary calculation employing different widths for the two subbands did not give significantly improved results even though electrical data seem to imply that the lower subband might have a wider bandwidth.[3]

Using the model just described, we have made a computer calculation of

$$F''_{\rm el}(T) \equiv \left[\frac{\partial^2 F_{\rm el}}{\partial(\delta E)^2} \right]_T \tag{6}$$

by evaluating $F_{\rm el}$ for values of δE from -1×10^{-4} eV to $+1 \times 10^{-4}$ eV in steps of 2×10^{-5} eV at each selected temperature between 300 and 650 K. The results are plotted in Fig. 4. From Eq. (4) and the usual expression for the elastic energy density of rhombohedral crystals in terms of strain components,[20] it can be shown that the

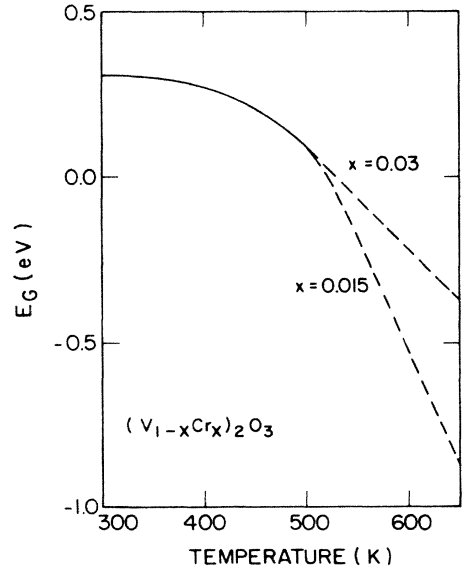

FIG. 3. Plot of the energy gap, E_G, as a function of temperature between 300 and 650 K for $(V_{1-x}Cr_x)_2O_3$ with $x = 0.015$ and 0.03. The solid curve is from Ref. 3 and the dashed curves above 500 K are chosen as described in the text.

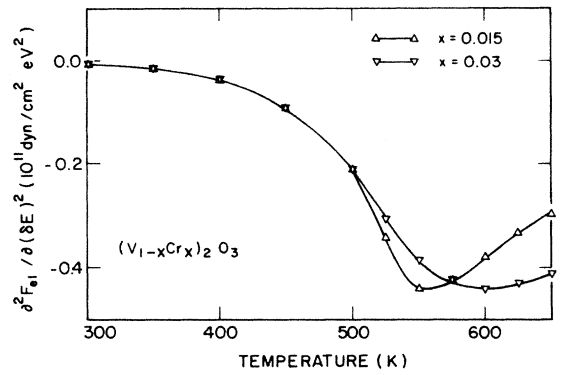

FIG. 4. Plot of $F''_{el}(T)$ [defined in Eq. (6)] as a function of temperature between 300 and 650 K for $(V_{1-x}Cr_x)_2O_3$ with $x=0.015$ and 0.03.

electronic contributions to the $C_{\mu\nu}$'s at temperature T relative to that at 300 K are given by

$$\Delta C^{el}_{11}(T)=A_1^2[F''_{el}(T)-F''_{el}(300)]=\Delta C^{el}_{12}(T)\ , \tag{7a}$$

$$\Delta C^{el}_{33}(T)=A_3^2[F''_{el}(T)-F''_{el}(300)]\ , \tag{7b}$$

and

$$\Delta C^{el}_{13}(T)=A_1A_3[F''_{el}(T)-F''_{el}(300)]\ , \tag{7c}$$

where the A_μ's are assumed to be independent of temperature. It is obvious that the $\Delta C^{el}_{\mu\nu}$'s in Eqs. (7a) and (7c) fulfill the conditions [Eqs. (3a) and (3b)] required by our experimental results. By least-squares fitting the $\Delta C^{el}_{\mu\nu}$'s to the $\Delta C_{\mu\nu}$'s for $(V_{0.985}Cr_{0.015})_2O_3$ in Fig. 2, the deformation potentials were found to be $A_1\simeq 3.6$ eV and $A_3\simeq 1.4$ eV. Very satisfactory agreement was obtained between the calculated and experimental ΔC_{11}'s as illustrated in Fig. 5. The fit for ΔC_{12}, ΔC_{13}, and ΔC_{33} are not shown here since they were of almost equal quality as can be expected from the fact that Eqs. (7) are consistent with experimental observations expressed in Eqs. (3). Also shown in Fig. 5 are the results of similar fitting for ΔC_{11} of $(V_{0.97}Cr_{0.03})_2O_3$ which yielded a value of 2.9 eV for A_1.

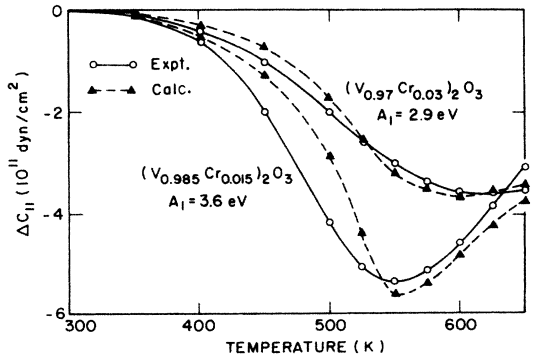

FIG. 5. Comparison between the experimental and calculated ΔC_{11}'s as a function of temperature between 300 and 650 K for $(V_{1-x}Cr_x)_2O_3$ with $x=0.015$ and 0.03. The calculated values are the electron-transfer contributions as given by Eq. (7a).

The anisotropy in the deformation-potential tensor, $A_\perp/A_{||}=A_1/A_3\simeq 2.6$ for $(V_{0.985}Cr_{0.015})_2O_3$, may be associated with the fact that the $e_g(\pi)$ subbands considered in our model are comprised of orbitals directed primarily towards neighboring metal atoms in the basal plane perpendicular to the c axis.[25] It is, therefore, expected that the shift of $e_g(\pi)$ bands are much more affected by the strain in the basal plane than that along the c axis. On the other hand, the smaller $A_\perp$ for $x=0.03$ than for $x=0.015$ may be understood from the phase diagram of the $(V_{1-x}Cr_x)_2O_3$ system,[2] since for $x>0.01$ increasing the Cr_2O_3 content (being equivalent to applying "negative" pressure) would drive the system away from the boundary of the pressure-induced, semiconductor- (insulator) to-metal transition, thereby making the compound more stable against the external stress.

The electron-transfer mechanism considered so far for the temperature dependence of the $C_{\mu\nu}$'s can also be utilized to understand some of the unusual pressure dependences of the $C_{\mu\nu}$'s previously observed in $(V_{1-x}Cr_x)_2O_3$ crystals; for example, the dramatic plunge of $\partial C_{11}/\partial P$ from $+12.9$ for $x=0$ (Ref. 26) to -21.6 and -7.9, respectively, for $x=0.015$ and 0.03 (Ref. 12). We assume that this unusually large difference in $\partial C_{11}/\partial P$ between the pure and Cr_2O_3-alloyed V_2O_3 is caused primarily by the pressure-induced change in the energy gap of the latter while the lattice component of $\partial C_{11}/\partial P$ changes little with the alloying of Cr_2O_3 into V_2O_3. We have further assumed that in the pressure range of our interest (up to 5 kbar) the energy gap of each $(V_{1-x}Cr_x)_2O_3$ crystal will decrease linearly with increasing pressure, i.e., $\partial E_G/\partial P=-\alpha$ where α is a constant. (This of course is qualitatively consistent with the existence of the pressure-induced, semiconductor-to-metal transition in these crystal.) Based on these assumptions we made a computer calculation of

$$C^{el}_{11}(P)=-A_1^2\left[\frac{\partial^2 F_{el}}{\partial(\delta E)^2}\right]_P \tag{8}$$

as a function of pressure at 300 K for each $(V_{1-x}Cr_x)_2O_3$ crystal using the values of deformation potentials deduced from the temperature dependence of ΔC_{11} (i.e., $A_1=3.6$ and 2.9 eV for $x=0.015$ and 0.03, respectively). The best

TABLE II. The difference between the pressure derivative of C_{11} for $(V_{1-x}Cr_x)_2O_3$ ($x=0.015$ and 0.03) and that for pure V_2O_3. The experimental values are taken from Ref. 12 and the calculated values are the electron-transfer contributions as described in the text.

	x	0.015	0.03
Expt.	$\left[\frac{\partial C_{11}}{\partial P}\right]_x-\left[\frac{\partial C_{11}}{\partial P}\right]_0$	-34.5	-20.8
Calc.		-33.3	-21.6

fit to the experimental values of $(\partial C_{11}/\partial P)_x - (\partial C_{11}/\partial P)_0$ for both $x=0.015$ and 0.03 were obtained with a single parameter of $\alpha=0.075$ eV/kbar as illustrated in Table II.

In conclusion, we have demonstrated that the electron-transfer mechanism can account for some of the anomalous temperature and pressure dependences we have found for various elastic constants of $(V_{1-x}Cr_x)_2O_3$ crystals with $x=0.015$ and 0.03.

ACKNOWLEDGMENTS

We are deeply indebted to the late Dr. H. R. Harrison of the Purdue University Materials Research Laboratory for the growth of the invaluable single crystals used in this research. This work was supported in part by the National Science Foundation via Materials Research Laboratory Program Grant No. DMR-80-20249.

[1]D. B. McWhan, T. M. Rice, and J. P. Remeika, Phys. Rev. Lett. **23**, 1384 (1969).
[2]D. B. McWhan and J. P. Remeika, Phys. Rev. B **2**, 3734 (1970).
[3]H. Kuwamoto, J. M. Honig, and J. Appel, Phys. Rev. B **22**, 2626 (1980).
[4]B. Belbeoch, R. Kleinberger, and M. Roulliay, J. Phys. Chem. Solids **39**, 1007 (1978).
[5]W. R. Robinson, Acta Crystallogr. Sect. B **31**, 1153 (1975).
[6]H. J. Zeiger, Phys. Rev. B **11**, 5132 (1975).
[7]C. Castellani, C. R. Natoli, and J. Ranninger, Phys. Rev. B **18**, 4967 (1978).
[8]M. Grodzicki, O. Jepsen, and O. Andersen (unpublished).
[9]D. N. Nichols, R. J. Sladek, and H. R. Harrison, Phys. Rev. B **24**, 3025 (1981).
[10]G. V. Chandrashekar and A. P. B. Sinha, Mater. Res. Bull. **9**, 787 (1974).
[11]H. Yang, R. J. Sladek, and H. R. Harrison, Solid State Commun. **47**, 955 (1983).
[12]H. Yang, R. J. Sladek, and H. R. Harrison, Phys. Rev. B **31**, 5417 (1985).
[13]S. A. Shivashankar, R. Aragon, H. R. Harrison, C. J. Sandberg, and J. M. Honig, J. Electrochem. Soc. **128**, 2472 (1981).
[14]Analyses performed by Galbraith Laboratories, Inc., P. O. Box 4187, Knoxville, TN 37921.
[15]E. P. Papadakis, J. Acoust. Soc. Am. **42**, 1045 (1967); H. J. McSkimin and P. Andreatch, *ibid.* **34**, 609 (1962).
[16]H. Yang, R. J. Sladek, and H. R. Harrison, Bull. Am. Phys. Soc. **28**, 252 (1983).
[17]S. C. Lakkad, J. Appl. Phys. **42**, 4277 (1971).
[18]H. V. Keer, D. L. Dickerson, H. Kuwamoto, H. L. C. Barros, and J. M. Honig, J. Solid State Chem. **19**, 95 (1976).
[19]R. W. Keyes, in *Solid State Physics,* edited by F. Seitz and D. Turnbull (Academic, New York, 1967), Vol. 20, p. 37.
[20]T. C. Chi and R. J. Sladek, Phys. Rev. B **7**, 5080 (1973).
[21]M. Born and K. Huang, *Dynamical Theory of Crystal Lattices* (Oxford University Press, London, 1954), p. 213.
[22]P. B. Miller and J. D. Axe, Phys. Rev. **163**, 924 (1967).
[23]H. Yang and R. J. Sladek, Phys. Rev. B **32**, 6634 (1985).
[24]A. Okamoto, Y. Fujita, and C. Tatsuyama, J. Phys. Soc. Jpn. **52**, 312 (1983).
[25]J. B. Goodenough, in *Progress in Solid State Chemistry,* edited by H. Reiss (Pergamon, New York, 1971), Vol. 5, p. 145.
[26]D. N. Nichols and R. J. Sladek, Phys. Rev. B **24**, 3155 (1981).